Can. J. Remote Sensing, Vol. 34, No. 3, pp. 320–332, 2008

Retrieving crown leaf area index from an individual tree using ground-based lidar data

Inian Moorthy, John R. Miller, Baoxin Hu, Jing Chen, and Qingmou Li

Abstract. Light detection and ranging (lidar) sensors, both at the terrestrial and airborne levels, have recently emerged as useful tools for three-dimensional (3D) reconstruction of vegetated environments. One such terrestrial laser scanner (TLS) is the Intelligent Laser Ranging and Imaging System (ILRIS-3D). The objective of this research was to develop approaches to use ILRIS-3D data to retrieve structural information of an artificial tree in a controlled laboratory experiment. The key crown-level structural parameters investigated in this study were gap fraction, leaf area index (LAI), and clumping index. Measured *XYZ* point cloud data from a systematically pruned tree were sliced to retrieve laser pulse return density profiles, which subsequently were used to estimate gap fraction, LAI, and clumping index. Gap fraction estimates were cross-validated with traditional methods of histogram thresholding of digital photographs (r^2 = 0.95). LAI estimates from lidar data were corrected for the confounding effects of woody material and nonrandom foliage distribution and then compared with direct LAI measurements (r^2 = 0.98, RMSE = 0.26). The methods developed in this research provide valuable lessons for application to field-level TLS data for structural parameter retrievals. Successful demonstration of analysis protocols to extract crown-level structural parameters like gap fraction, LAI, and clumping index from TLS data will be important for detailed assessments of 3D canopy radiative transfer modeling and likely will lead to more robust inversion algorithms.

Résumé. Les capteurs lidar (« light detection and ranging »), que ce soit au niveau terrestre ou aéroporté, se sont avérés depuis peu des outils utiles pour la reconstruction 3D des environnements végétalisés. Le système ILRIS-3D (« Intelligent Laser Ranging and Imaging System ») est l'un de ces systèmes SLT (scanneur laser terrestre). L'objectif de cette recherche était de développer des approches pour l'utilisation des données 3D de ILRIS pour l'extraction de l'information structurelle d'un arbre artificiel dans le cadre d'une expérience contrôlée en laboratoire. Les paramètres structurels clés de la couronne examinés dans cette étude étaient les fractions de trous, l'indice de surface foliaire (LAI) et l'indice d'agrégation. Les données mesurées du nuage de points *XYZ* dérivés d'un arbre systématiquement taillé ont été découpées pour extraire les profils de densité des retours d'impulsion laser, qui furent utilisés par la suite pour estimer les fractions de trous, le LAI et l'indice d'agrégation. Les estimations de fractions de trous ont été co-validées à l'aide des méthodes traditionnelles de seuillage d'histogramme d'images numériques (r^2 = 0,95). Les estimations de LAI dérivées des données lidar ont été corrigées pour les effets confusionnels dus aux matériaux ligneux et à la distribution non aléatoire du feuillage, puis comparées aux mesures directes de LAI (r^2 = 0,98, RMSE = 0,26). Les méthodes développées au cours de cette recherche apportent des leçons utiles pour l'application des données de SLT acquises au sol à l'extraction des paramètres structurels. La démonstration réussie de protocoles d'analyse pour l'extraction des paramètres structurels de la couronne tels que les fractions de trous, le LAI et l'indice d'agrégation à partir des données de SLT deviendra importante pour les évaluations détaillées de modélisation 3D du transfert radiatif du couvert et conduira vraisemblablement à la mise au point d'algorithmes d'inversion plus robustes.
[Traduit par la Rédaction]

Introduction

The spatial organization of above-ground plant material, within a forest canopy, plays an important role in controlling photon–vegetation interactions, which in turn influence functional activities such as photosynthesis and evapotranspiration. The ability to describe forest canopy structure involves the characterization of the shape, position, size, and orientation of vegetative elements. Furthermore, the organization of the vegetative elements can be evaluated at

Received 17 December 2007. Accepted 5 May 2008. Published on the *Canadian Journal of Remote Sensing* Web site at http://pubs.nrc-cnrc.gc.ca/cjrs on 29 August 2008.

I. Moorthy.[1] Centre for Research in Earth and Space Science (CRESS), Petrie Science and Engineering Building, York University, 4700 Keele Street, Toronto, ON M3J 1P3, Canada.

J.R. Miller and B. Hu. Department of Earth and Space Science and Engineering, Petrie Science and Engineering Building, York University, 4700 Keele Street, Toronto, ON M3J 1P3, Canada.

J. Chen. Department of Geography and Planning, Sidney Smith Hall, St. George Campus, University of Toronto, 100 St. George Street, Toronto, ON M5S 3G3, Canada.

Q. Li. Canada Centre for Remote Sensing, Natural Resources Canada, 588 Booth Street, Ottawa, ON K1A 0Y7, Canada.

[1]Corresponding author (e-mail: moorthy@eol.esse.yorku.ca).

 © 2008 CASI

multiple spatial scales (i.e., individual tree, forest canopy, and ecosystem). Large-scale canopy architecture is often described using spatially integrating properties such as leaf area index (LAI), which is the total one-sided area of leaf tissue per unit horizontal ground area (Watson, 1947). To account for nonflat leaves such as needles, this definition was modified by Chen and Black (1992) to half the total developed area of leaves per unit ground surface area. LAI is a primary variable employed in ecosystem models that quantitatively characterize energy exchanges between the atmosphere and the canopy. However, directly measuring LAI involves destructive sampling and time-consuming methods (Lang et al., 1985), thus spatially extensive in situ measurements to characterize large-scale heterogeneity are not feasible (Jonckheere et al., 2004). To overcome such obstacles, various approaches have been developed to indirectly measure canopy structure, involving optical instruments (i.e., DEMON, LAI-2000, tracing radiation and architecture of canopies (TRAC)) and models (Lang et al., 1985; Welles and Norman, 1991; Chen and Cihlar, 1995). These instruments measure gap fraction, which is the integrated value of the gap frequency over a given domain (Weiss et al., 2004). Gap fraction can then be inverted to retrieve LAI values, or more specifically plant area index (PAI), since leaf and woody material are not distinguished from one another. Also, LAI retrievals that are based on random leaf distribution models can be erroneous, since actual canopy foliage is not randomly distributed (Jonckheere et al., 2006). In addition, optically based techniques are indirect methods that rely on vegetation spectral characteristics, which not only are influenced by tree–leaf structure but also are affected by viewing–illumination geometries. With the recent introduction of laser technology in the field of remote sensing, there is now potentially a means of directly acquiring a comprehensive mathematical description of tree structure (van der Zande et al., 2006). Light detection and ranging (lidar) instruments use the time-of-flight (TOF) principle to measure the distances of objects based on the time interval between laser pulse exitance and return, upon reflection from an object. Recent studies have illustrated the ability to derive forest canopy structure from airborne lidar observations (Lefsky et al., 2002; Naesset, 2002; Parker et al., 2001; Riano et al., 2004). At the ground level, tripod-mounted lidar units or terrestrial laser scanners (TLS), commonly used for mining, urban planning, and surveying applications, can be used to rapidly obtain three-dimensional (3D) spatial datasets (Lichti et al., 2002). The application of TLS data for ecological monitoring is now at the forefront of active remote sensing research. Scientists have begun to recognize such lidar systems can now be deployed in a forest environment to quickly digitize structural information of tree crowns, potentially replacing laborious, time-consuming, and often relatively inaccurate manual field measurements. Radtke and Bolstad (2001) derived the vertical distribution of vegetation structure within broad-leaved forests by acquiring vertically emitted laser beams from the forest floor, using a commercially available laser rangefinder. By mounting a laser ranging system on a pan–tilt platform, Lovell et al. (2003) cross-validated laser-derived LAI estimates with those obtained by hemispherical photography to within 8%. More recently, TLS data have been used to estimate other photosynthetically significant parameters such as plant area densities (Takeda et al., 2008) and the ratios of woody to total plant areas (Clawges et al., 2007). Additional research that focused on the measurement and segmentation of tree stem diameters and branching structures has also been conducted (Henning and Radtke, 2006; Hopkinson, 2004; Thies et al., 2004; Watt and Donoghue, 2005). Although the delineation of stem diameters is tree specific, the retrievals of LAI are spatially integrated for the entire canopy. Laser technology offers the potential of calculating LAI at the individual crown level provided that 3D point cloud data can be acquired for isolated crowns. It is in this context that this paper describes the acquisition and analysis of 3D TLS data for an individual artificial *Ficus* tree.

Controlled laboratory experiments were conducted using an artificial *Ficus* tree, which was systematically pruned to illustrate the impact of various stages of foliage cover, from full "leaf-on" to complete "leaf-off," on the laser pulse returns. A slicing routine was developed to analyze the lidar data and extract pertinent tree crown structural information, namely crown-level gap fraction and LAI. Often, within the remote sensing community, these two parameters are considered or modeled at the canopy scale. However, due to the precision of laser scanning systems and the flexibilities of controlled laboratory experiments, these two parameters can now potentially be estimated at an individual crown scale. It was the objective of this research to explore innovative methods of retrieving gap fraction and LAI in a controlled environment, from which lessons could be applied to field-level TLS data.

Experimental data acquisition and processing

Intelligent laser ranging and imaging system (ILRIS-3D)

The Intelligent Laser Ranging and Imaging System (ILRIS-3D), developed by Optech Incorporated, Toronto, Canada, is a tripod-mounted surveying tool with a 40° × 40° field of view and a scanning range of 3 m to beyond 1000 m (**Table 1**). The ILRIS-3D is robustly designed for field use and operates at a scanning rate of 1500 laser pulses per second. The class 1 laser (eye safe) has a wavelength of 1535 nm. The spot spacing between laser pulses is 0.026 mm × R, where R is the range distance in metres. The laser pulse diameter is 12.7 mm at exitance and degrades at a rate of 0.17 × R. The system has a beam divergence of 0.00974° (0.17 mrad) and a minimum spot size of 0.00115° (0.02 mrad). The high-speed counter within the ILRIS-3D measures the TOF from the start of a laser pulse to the return of that pulse. The time measurement (t) is then converted to distance (d) using the relationship $d = ct/2$, where c is the speed of light. The acquired dataset, for a given scan, consists of *XYZ* and intensity point cloud data, a low-resolution digital image of the captured screen, and field notes entered during the scan by the operator. The

© 2008 CASI

Table 1. Technical specifications of the Optech Incorporated ILRIS-3D.

Dynamic scanning range	3–1500 m to an 80% target; 3–800 m to a 40% target; 3–350 m to a 4% target
Data sampling rate	1500 pulses/s
Beam divergence	0.00974°
Minimum spot step (azimuthal and zenith axes)	0.00115°
Laser wavelength	1535 nm
Laser class	Class 1 (eye safe)
Scanner field of view	40° × 40°
Control interface	T3 palm pilot
Power supply	24 V DC
Scanner dimensions	320 mm × 320 mm × 220 mm (length × width × height)
Scanner weight	13 kg
Data storage	1 Gb removable compact flash memory card
Digital camera	Externally mounted Nikon D50 and 20 mm lens

acquired data can be recorded for either first pulse returns or last pulse returns. All data are written directly to an on-board removable flash card. Postprocessing of the data was done using a software package known as Polyworks (version 9) from InnovMetric. ILRIS-3D data were complemented with a high-resolution digital photograph obtained with a Nikon D50 digital camera mounted to the system.

Laser scanning of artificial tree

The ILRIS-3D, mounted on a survey tripod, was used to acquire point clouds of an artificial *Ficus* tree (**Table 2**) in a controlled laboratory environment. The artificial tree was affixed to a rotating platform, allowing multiple perspectives of the tree from a stationary viewpoint. First pulse returns were recorded to yield point cloud files that show the *XYZ* coordinate of each detected element. First pulse data measure the range of the first object encountered, which in this experiment was the foliage and stem elements of the tree. The distance between the tree stem location and the ILRIS-3D was kept constant at 10 m, and all scans were acquired at an angular (x–y) resolution of 2 mm at 10 m (assume parallel laser). After the scan, the tree was rotated 90° for subsequent scans from three other perspectives. Once four perspectives of the tree were measured, leaf samples were pruned from the tree. To provide a range of structural conditions, the tree was systematically defoliated to decrease the leaf count from 970 leaves (full foliage) to 0 leaves in 10 stages (**Table 3**). Although no precise criteria were employed to determine which leaf gets pruned and which does not, the experiment followed the guideline of pruning two leaves from each branch for the first six steps of defoliation and one leaf per branch for the last three steps. This guideline yielded an approximate symmetrical distribution of clipped leaves after each pruning stage. The four perspectives and 10 steps of leaf cover yield a total of 40 lidar scans of the artificial tree. The 3D point cloud from one perspective at the different levels of leaf cover is shown in **Figure 1**. At each defoliation step, the leaf inclination angle of all the pruned leaves was measured. All the pruned leaves of a given defoliation step were stored together. The individual leaf area of a subset of leaves (n = 100), 10 leaves at each defoliation step, was measured using a commercial flatbed scanner.

Table 2. Artificial tree characteristics.

Tree height	1.7 m
Crown dimensions	0.85 m × 0.90 m (length × width)
Trunk diameter	0.15 m
Leaf dimensions	0.09 m × 0.05 m (length × width)
Materials	Silk-screened polyester leaves

Table 3. Leaf count at each step of tree defoliation.

Step No.	No. of leaves	Crown LAI
1	970	4.90
2	850	4.29
3	718	3.63
4	580	2.93
5	448	2.26
6	310	1.57
7	172	0.87
8	106	0.54
9	58	0.29
10	0	0

Processing 3D lidar point clouds

Preprocessing of the 3D lidar data was conducted to omit all laser pulse returns that were extraneous to the target. Using Polyworks, a region of interest was delineated around the tree and all laser pulse returns outside of the region (i.e., from background wall, ground, etc.) were excluded. Exclusion of all non-tree laser pulse returns was a straightforward process because they were visually distinguishable in the Polyworks software environment. After omitting the extraneous points, the resultant 3D point cloud was saved in ASCII text format and served as the input to a slicing algorithm that was used to plot profiles of the lidar data. Data were processed using the following steps: (1) read in the *XYZ* ASCII text file from one

© 2008 CASI

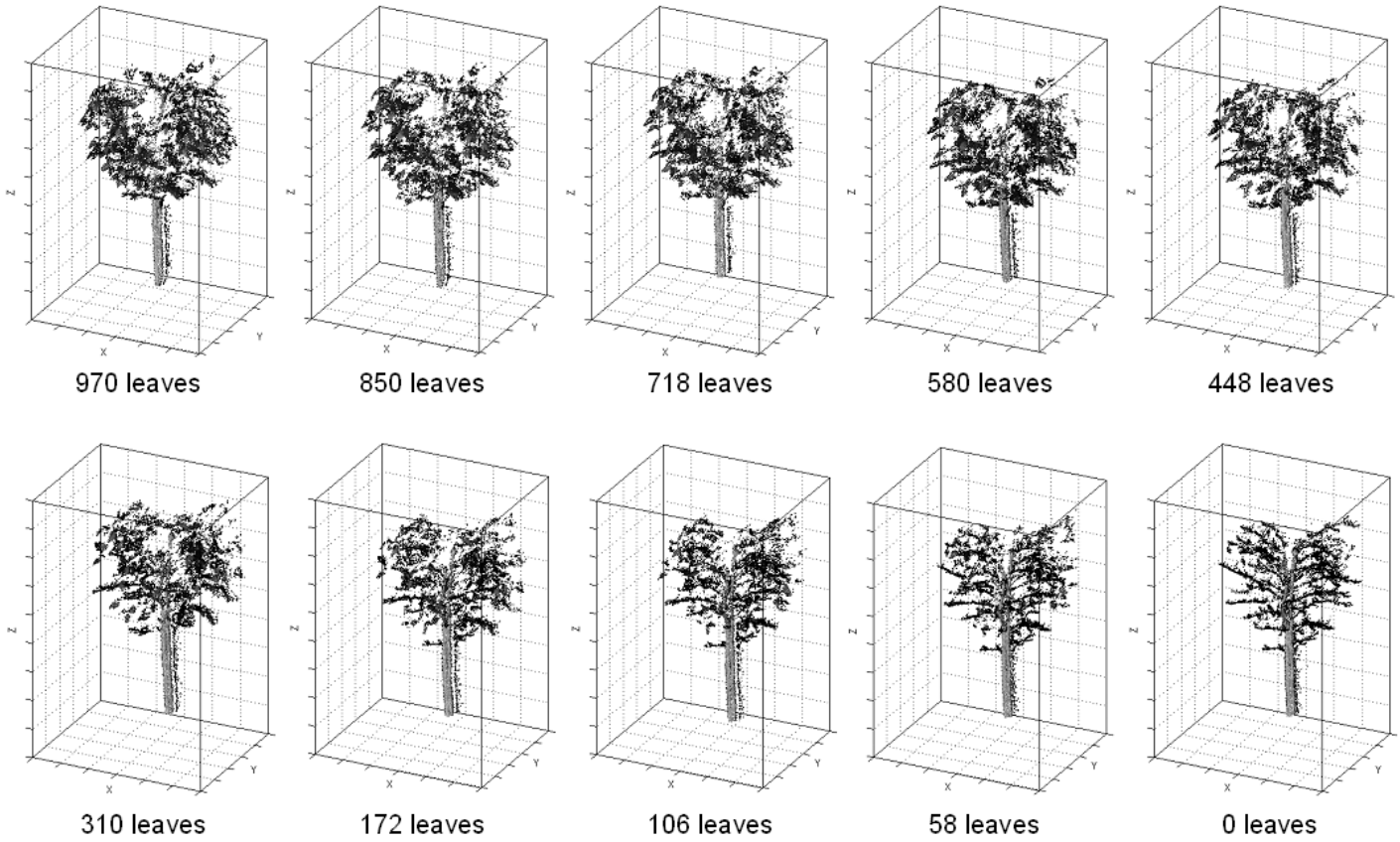

Figure 1. ILRIS-3D scans of the artificial tree were acquired at each step of the systematic defoliation from 970 leaves to 0 leaves. Angular scan resolution was 2 mm, and the laser spot diameter was 13.7 mm with the tree positioned at a distance of 10 m from the scanner. Perspective 1 is illustrated here.

ILRIS-3D scan; (2) determine the nearest (*Y*-min) and farthest (*Y*-max) laser pulse returns along the range direction (*Y*-axis); (3) slice the data between the two extreme returns by a user specified number of intervals; (4) tabulate all the laser pulse returns that fall within one interval; (5) calculate the centre of momentum for the laser pulse returns within one interval (*X* and *Z* mean); (6) use Delaunay triangulation to draw topological triangles between detected laser pulse points within a predefined slice; (7) sum up the calculated areas of each of the topological triangles within a slice; (8) use the cumulative area from step 7 and calculate the radius of a circle with the equivalent area (assumption that crown is spherical); (9) determine laser pulse return density using the tabulated number of points and the area of the polygon within a slice; and (10) output results to an ASCII file.

The resultant output file yielded the following information: start of interval (*Y*-min), end of interval (*Y*-max), *X* mean, *Z* mean, number of pulses, polygon area, equivalent circle radius, and pulse density. The algorithm allows a quick profiling of the point cloud by displaying the fraction of returned laser pulses as a function of distance from the scanner. Determining these profiles is an efficient means of evaluating tree structural properties, which cannot be easily obtained using the tools provided with the Polyworks software platform.

Since the data are from a TLS, the profiles show pulse returns as a function of distance into the crown from the front edge to the back, unlike retrievals from airborne lidar systems, which typically show a top-down perspective of a tree. It is important to note that the 3D point density is variable due to the physical pulse–object interactions and the intrinsic characteristics of the laser (van der Zande et al., 2006). Since first pulse return measures the reflection of the first object it encounters, the spatial information of elements located behind the object is not available due to the shadow effect (van der Zande et al., 2006). As a result, the multiple perspectives acquired in this experiment help to effectively minimize the influence of shadows and provide a more complete 3D representation of the crown. Such comprehensive coverage is not practically feasible in field environments, but such benefits and lessons at the laboratory scale must first be explored. The effect of intrinsic scanner properties on the pulse return density was also considered using a methodology recently reported by Danson et al. (2007), who developed a laser scanner model (for the Riegl LMZ210i) to effectively predict the number of laser pulse returns based on inherent characteristics of the TLS. Since the TLS system does not record laser misses, it is necessary to quantify the number and direction of all laser pulses in a scan, which is dependent on resolution, scanning

© 2008 CASI

geometry, and line and frame scan angle range (Danson et al., 2007). Thus, generating a laser scanner model for the ILRIS-3D to predict the number of laser pulse returns for a given area is needed. Unlike the two-axis scanning mechanism of the Riegl LMZ210i, the ILRIS-3D is a simplified frame viewing TLS. Consequently, the need for multiple coordinate system transformations to build the pulse density prediction model is not necessary. The user specifies the scan resolution (i.e., the spacing between laser pulses) at the time of data acquisition, and that resolution degrades linearly with range distance. Therefore, it is possible to determine the exact number of laser pulses that "hit" a target of known area at any given range from the ILRIS-3D. Furthermore, under the conditions that the target is (*i*) normal to the collimated laser pulses and (*ii*) 100% reflective, the number of returned laser pulses should equal the number of pulses emitted. This idealized perspective also assumes that there are no losses of laser pulses to the surroundings, by scattering or absorption. Consequently, the theoretical laser pulse density as a function of distance for varying scan resolutions can be established (**Figure 2**). Differences between the predicted pulse density and the measured values of the tree crown can be used to retrieve architectural parameters such as crown-level gap fraction. The ratio of the measured pulse density to the theoretical density at the same distance from the scanner yields the percent cover:

$$\text{(measured pulse density)/(theoretical pulse density)} = \text{percent cover} \quad (1)$$

Gap fraction is the probability of a pulse being transmitted through the vegetated target without encountering any objects. Therefore, the gap fraction P for the view direction θ can then be obtained based on the principle that

$$1 - \text{(percent cover)} = P(\theta) \quad (2)$$

Therefore the return of an emitted laser pulse means 0% gap, and lack of return for a given pulse means 100% gap. Since the ILRIS-3D is a frame-viewing scanner, the view direction is fixed, and the resultant retrievals can be more specifically labeled as monodirectional gap fraction. It is important to note that target reflectivity and orientation of target elements relative to the pulse direction can lead to possible errors of inclusion or omission in the recorded number of laser pulses. For example, a particular element within the path of the laser beam needs to have a high enough reflectivity to produce a return signal that can be recorded. If the reflected signal does not exceed the scanner intrinsic noise threshold, then return pulse is not recorded, thereby erroneously indicating that a gap is present (Danson et al., 2007). Despite the range dependency on the ability to detect gaps, the knowledge of sensor intrinsic properties, such as the degradation of angular (*XY* plane) resolution with distance, allows the normalization of this dependency. This investigation employs an approach that is similar to that of traditional methods (i.e., hemispherical photography), where indirect estimates of LAI are determined through direct measurements of gap fraction as follows:

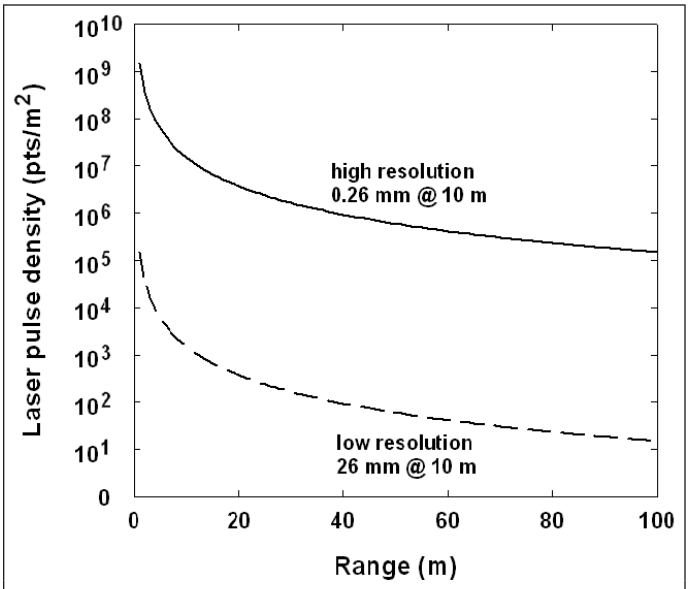

Figure 2. Knowledge of the scanning configuration parameters, mainly scan resolution, can be used to determine the theoretical pulse return density (points/m^2) from a solid object (assume no losses due to scattering or absorption during travel path) at any distance. Highest resolution capable of the ILRIS-3D is 0.26 mm at 10 m.

$$P(\theta) = \exp\left[\frac{-G(\theta)\,\Omega\,\mathrm{LAI}}{\cos(\theta)}\right] \quad (3)$$

where $G(\theta)$ is the G function (mean projection of unit foliage area), Ω is the clumping index (nonrandomness factor), and $\theta = 0$.

A G function value of 0.5 was used in the experiment, based on our measurements of the inclination angle of each leaf as it was excised during the laboratory experiment. Currently, the widely accepted reasons for errors in LAI estimation are (*i*) the contribution of nonleafy material (i.e., stems, branches); and (*ii*) the nonrandom distribution of foliar elements as described by Ω, or the clumping index (Breda, 2003). Gap fraction based methods of determining LAI cannot directly distinguish between green and nongreen materials (i.e., stems, trunks, branches, senescent leaves, etc.). The amount of wood material and its spatial organization can significantly alter LAI estimates using optical instruments. Therefore, alternative terms such as vegetation area index (VAI) (Fassnacht et al., 1994) and plant area index (PAI) (Neumann et al., 1989) have been proposed to label retrievals using gap fraction methods. However, to appropriately link LAI to canopy functional processes, it is necessary to specifically target the green photosynthetic components and account for woody material contributions (Weiss et al., 2004). Chen (1996) introduced the woody area index parameter α, based on intensive destructive measurements, into the calculations of LAI. Furthermore, the deviation of the foliage arrangement from a random distribution, more commonly known as the clumping index Ω,

© 2008 CASI

Table 4. Laser pulse return counts for ILRIS-3D scans.

No. of leaves	Perspective 1	Perspective 2	Perspective 3	Perspective 4
980	49 215	48 874	49 201	48 672
850	46 019	47 743	48 480	49 396
718	44 771	46 208	45 223	46 283
580	44 283	45 868	43 417	44 133
448	41 597	42 207	41 095	42 839
310	38 802	40 525	37 941	40 569
172	34 467	36 036	36 642	36 644
106	31 503	33 297	32 120	34 405
58	29 048	32 179	30 333	32 584
0	24 258	29 666	24 779	29 248

is a bias in LAI estimation that must be resolved. The term effective LAI (L_e) was used to describe the product of Ω and LAI. The clumping index is equal to unity for a random foliage distribution and deviates from unity as the distribution becomes more clumped. The relationship between clumping index, woody material (α), and true LAI (Equation (4)) was proposed by Chen and Black (1992), where

$$\mathrm{LAI} = \frac{(1-\alpha)L_e}{\Omega} \tag{4}$$

From Chen and Cihlar (1995), the clumping index can be calculated by

$$\Omega = \frac{\ln[P_m(\theta)]}{\ln[P_o(\theta)]} \tag{5}$$

where $P_m(\theta)$ is the measured gap fraction, and $P_o(\theta)$ is the imaginary gap fraction with a random spatial distribution.

The unique data (i.e., multiple perspectives and varying leaf densities) collected in this experiment using the ILRIS-3D allow the quantification of both of these sources of discrepancies (α and Ω). The contribution of α to the LAI was determined using the scan of the artificial tree in the leaf-off state. Laser pulse densities of the woody material can be subtracted from the other leaf-on states to get a direct estimate of the green material component. The clumping index was determined by comparing the measured gap fraction for the tree versus the gap fraction of a simulated random laser pulse distribution within the same boundary space (Equation (5)). The determination of these two sources of discrepancies allows the accurate retrieval of LAI from gap fraction estimates and extends the experiments conducted and described in Danson et al. (2007).

Experimental results and discussion

Extracting structural parameters: crown-level gap fraction

A total of 40 ILRIS-3D scans were acquired from the artificial tree (4 perspectives × 10 steps of leaf cover). The varying perspectives all exhibit a steady decrease in the number of laser pulse counts as the amount of leaf material was decreased (**Table 4**). Each scan was separated into 50 slices of approximately 2 cm thickness along the range direction (*y* axis). The slicing routine is capable of slicing the *XYZ* point cloud data into as many slices as required by the user. Increasing the number of slices (i.e., decreasing slice thickness) provides more detailed profiles of the laser pulse returns from the tree crown. However, other issues such as computational time must be considered when selecting the number of required slices. In this investigation 2 cm thick slices were chosen, for quick computation time, without compromising the resolution of the retrieval of along-range profiles. Based on the tabulation of points and the calculation of area for a given slice, the fractional laser pulse return and the laser pulse return density as a function of distance into the crown were determined (**Figure 3**). The location of the highest fractional laser pulse

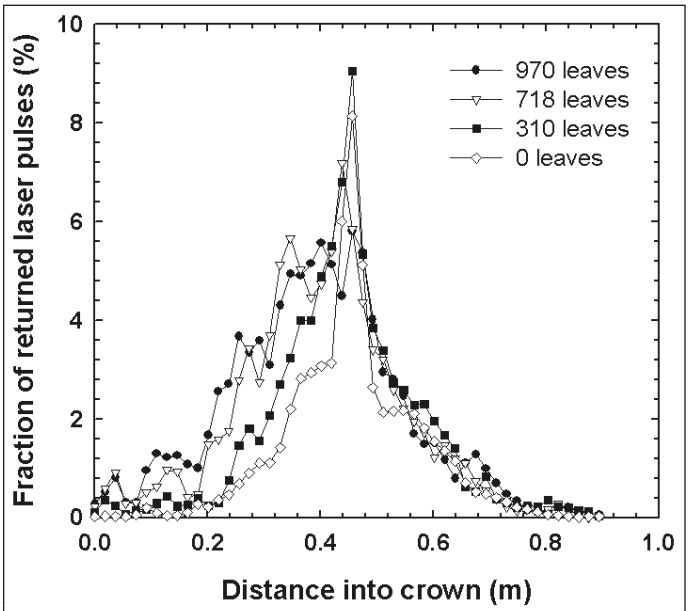

Figure 3. Slicing of the *XYZ* point cloud into 2 cm thick slices yields laser pulse distribution profiles as a function of crown distance. Decreasing the leaf material results in a lower fraction of returned laser pulse in the front half of the tree. Minimal changes were observed in the back half of the tree due to shadowing.

© 2008 CASI

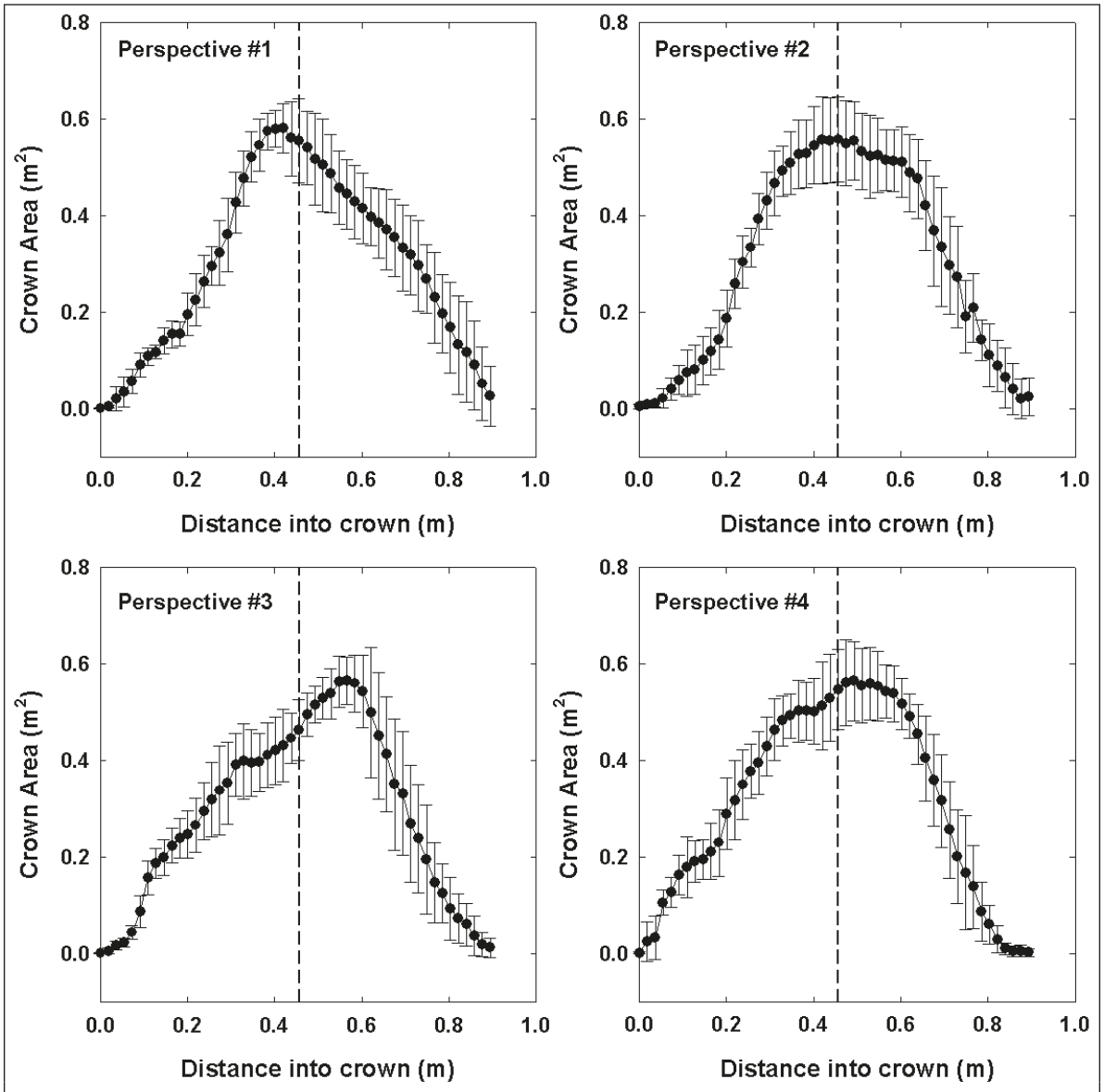

Figure 4. Mean crown area (from 10 steps of leaf cover) as a function of distance for the four perspectives of the artificial tree. Errors bars represent one standard deviation from the mean.

return for any given perspective corresponded with the stem location. The stem and branch elements of the tree play a significant role in the number of laser pulse returns. As the number of leaves was reduced, the fraction of laser pulse returns on the front half of the tree decreased, with minimal changes observed in the back half of the tree. Defoliation of the tree can be detected at the front half of the tree, as observed by the high degree of variability before the stem location. However, leaf and woody elements at the front half of the tree were intercepting the laser pulses, and thus obscuring the return of laser pulses from elements in behind. In other words, laser pulse shadowing increases with increasing LAI, but beyond the stem location the crown can be considered optically thick. Despite the efforts of azimuthal symmetry in the pruning process, obstructions and shadowing inhibit the ability to accurately retrieve leaf material in the back half of the tree. Thus, rotating the tree and collecting data from multiple perspectives provides sufficient information about all sides of the crown for accurate structural parameter extraction.

During the separation of the point cloud into slices, a Delaunay triangulation algorithm was used to calculate crown area. The triangulation was computed on each individual slice to determine crown area as a function of distance from the four different perspectives at all leaf count levels (**Figure 4**). This triangulation method was compared to another approach where the maximum radius of each slice (based on Euclidean distance of point distribution) was estimated. Area calculations were subsequently determined using the derived maximum radius, assuming a spherical crown. Due to the variability in point spatial distribution along the range direction, the maximum-

© 2008 CASI

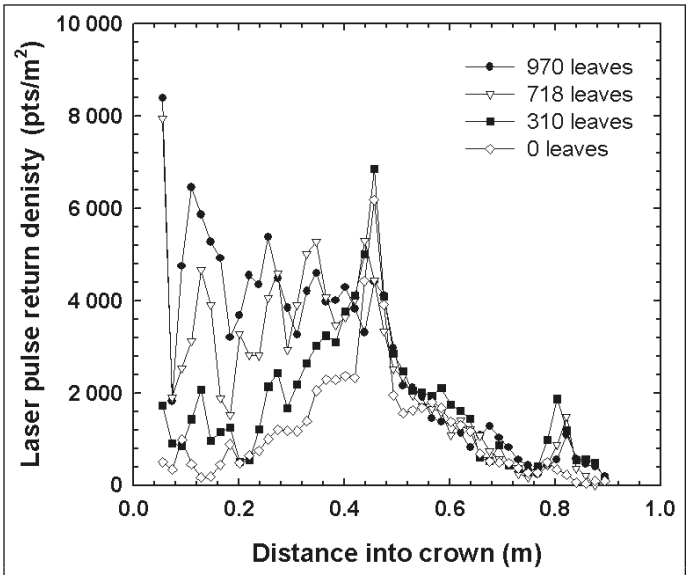

Figure 5. Pulse return density (points/m^2) as a function of distance into the crown was determined based on slice area calculations and tabulation of laser returns. Changes in leaf density influenced retrievals in the front half of the tree, with negligible difference beyond stem location.

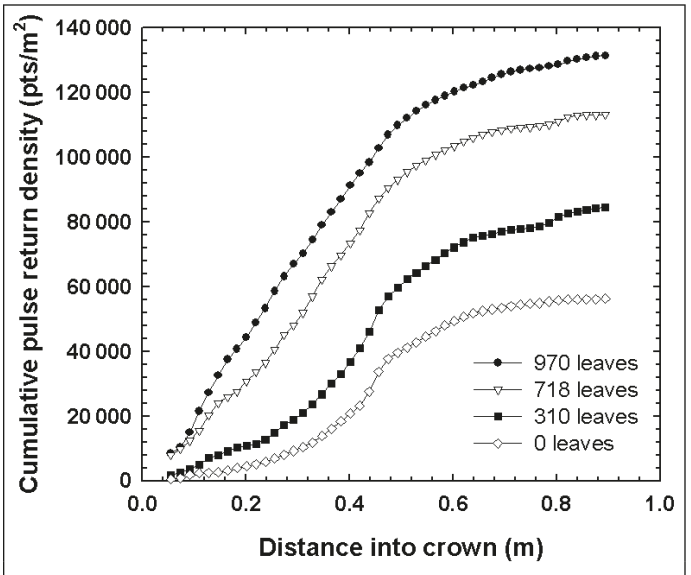

Figure 6. Summation of the laser pulse return densities from the front and back halves of the tree yields a cumulative pulse density (points/m^2) for the entire crown. The crown cumulative densities decrease as the leaf count decreases and are evaluated against the theoretical density for gap fraction estimation.

radius approach tended to overestimate crown area, which consequently underestimated laser pulse return density. The triangulation technique was more representative of the slice area because it considered all points within the slice and inherently accounts for the spatial distribution. Crown area retrievals from the different perspectives reveal the relative symmetry of the artificial tree (**Figure 4**). In other words, since perspectives 1 and 3 are opposing views of the crown, their area profiles along the range direction mirror one another. Upon calculation of the slice area and previous tabulation of the number of laser pulse returns per slice, density distributions can now be determined. As expected, the laser pulse return densities decrease as more leaves are pruned from the tree (**Figure 5**). The shadow effect of laser scanner data is also evident when laser pulse densities are calculated as a function of distance into the crown. Furthermore, to determine cumulative pulse density (**Figure 6**) we would sum the return density from the front side (up until stem location) of one perspective, with its opposing viewpoint, effectively joining two halves of the tree. The cumulative pulse return densities decrease as leaf count decreases. At the laboratory level we were capable of acquiring multiple perspectives, thereby permitting such a technique of integrating two halves of the crown. It is important to note that, although this approach is applicable in a controlled laboratory environment, it is potentially ineffective in the field, where acquiring more than one perspective of a tree may not be feasible due to obstructing elements in a stand of trees. Consequently, it is important to test the validity of this assumption by determining if an extrapolation from single-view data to retrieve full crown information is feasible. Comparing this cumulative point density from the tree with the sensor intrinsic theoretical density at the same range yields an estimate of crown gap fraction. To cross-validate gap fraction retrievals from TLS data, a more conventional dataset was acquired. High-resolution digital photographs, simultaneously acquired with ILRIS-3D scans, were used to estimate crown-level gap fraction. Histogram thresholding was employed on a binary representation of the photographs using standard image processing software to assess gap fraction (**Figure 7**). This methodology follows a protocol similar to that for hemispherical photography, which has already been shown to agree well with lidar-derived gap fraction retrievals (Danson et al., 2007; Hopkinson and Chasmer, 2007; Morsdorf et al., 2006). Although this optically based method using digital photography is an indirect approach, it provides a practical cross-validation dataset.

To address the value of multiperspective ILRIS-3D data of the tree crown, the comparisons between lidar-based gap fraction and photography-based estimates were done using two methods. The first assessment used the laser pulse return from one perspective (i.e., one half of the tree) and duplicated the back half, working under the assumption that the tree is completely symmetric (**Figure 8a**). The second assessment of gap fraction utilized the information from one half coupled with the data from the opposing perspective to effectively generate a full 3D representation of the artificial crown (**Figure 8b**). The experiments show that having true ILRIS-3D information from both halves of the crown significantly improves crown-level gap fraction estimates. In certain cases, the procedure of duplicating the back half using the front half laser pulse returns leads to an overestimation–saturation of points, thereby producing negative gap fraction values. In other words, there were more laser pulse returns than theoretically

© 2008 CASI

Figure 7. High-resolution digital photographs acquired at every defoliation step (shown here on first row, 970 leaves; second row, 58 leaves) were converted to binary images. Spectral thresholding techniques were used to calculate crown gap fraction based on the ratio of white to black pixels.

possible when tree structural symmetry was assumed and the back half was mimicked. The input of actual measured data from the back half corrected this problem and yielded better retrievals, when compared to traditional photographic methods. Since four perspectives were acquired, this effectively provides two complete 3D representations of each foliage step, when opposing views are merged. Therefore, 20 estimates of gap fraction for the tree were generated, and the estimates ranged from 1% at full foliage state to 64% at the zero leaf state. A 64% gap fraction at the leaf-off state indicates that the woody material of the tree is a significant contributor to the number of laser pulse returns. The relative contribution of woody material to gap fraction plays an important role in LAI estimation.

Crown-level leaf area index

After the estimation of gap fraction from the ILRIS-3D point clouds, the focus of the investigation shifted to retrieving LAI values. The systematic defoliation of the artificial tree provided a large range of LAI conditions. Ten pruned leaves from each of the 10 steps were scanned using a commercial flatbed scanner. A mean leaf area of 28 cm^2 was measured, with a variance of 5 cm^2 for the 100 leaf samples. The low variance in leaf area is due to the fact that this is an artificial tree. With the knowledge of not only the number of leaves, but also the leaf area, direct estimates of LAI were calculated. Based on the truth measurements, crown-level LAI values for the tree ranged from 0 to 4.9. LAI estimates from the ILRIS data were obtained, while accounting for the leaf inclination angle distribution, and compared with the actual LAI (**Figure 9**). Based on the gap fraction observations, initial LAI retrievals ranged from 0.8 to 8.7. Despite the strong correlation (r^2 = 0.95) between the estimated and truth measurements, there was still a large discrepancy in the estimates (root mean square error (RMSE) = 1.13). This disagreement is primarily due to the inclusion of the nongreen elements in the gap fraction. The stem and branches of the artificial tree are significant contributors to the laser pulse returns and the observed gap fraction. Therefore, these initial estimates of LAI, which include the woody material contribution, are more properly termed plant area index or PAI. Correcting for the woody material fraction α requires a subtraction of the cumulative laser pulse density of the leaf-off state from all other leaf-on states. Once this correction factor is applied, the LAI estimation errors decreased (RMSE = 0.68), and a more 1:1 relationship was observed (**Figure 10**). Once again, the flexibilities of a laboratory experiment allow lidar

© 2008 CASI

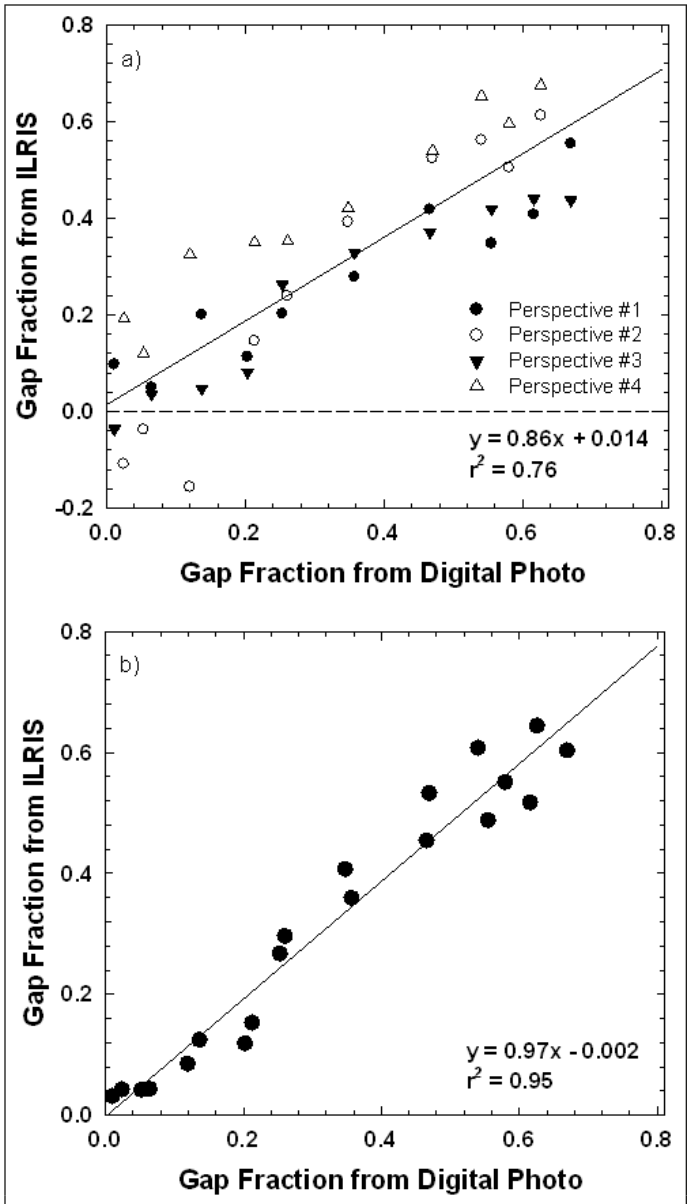

Figure 8. ILRIS-3D-derived gap fractions were compared with measured values (from digital photography) by (a) replicating individual perspectives (n = 40) (i.e., assume symmetrical tree), and (b) merging point densities from two opposing perspectives (i.e., perspectives 1 + 3 and perspectives 2 + 4) (n = 20).

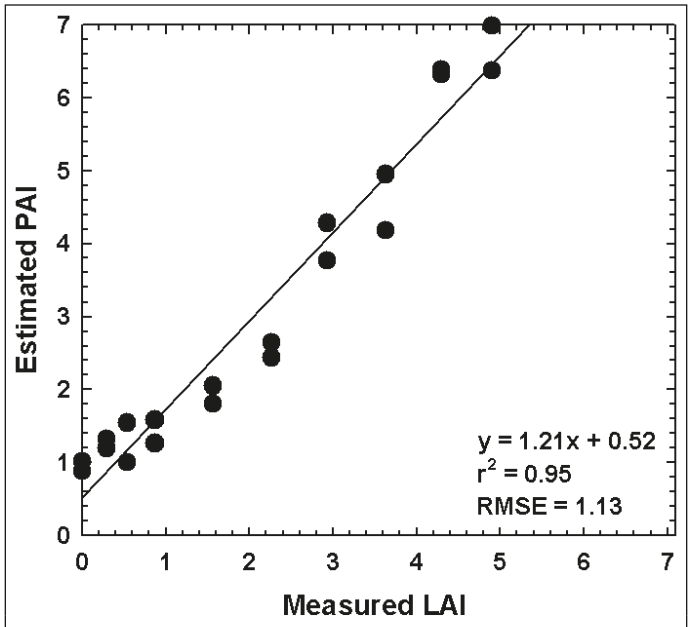

Figure 9. Estimated PAI from ILRIS-3D compared with actual LAI (scanned leaf clippings) reveals good agreement (r^2 = 0.95) but inaccurate estimates (RMSE = 1.13).

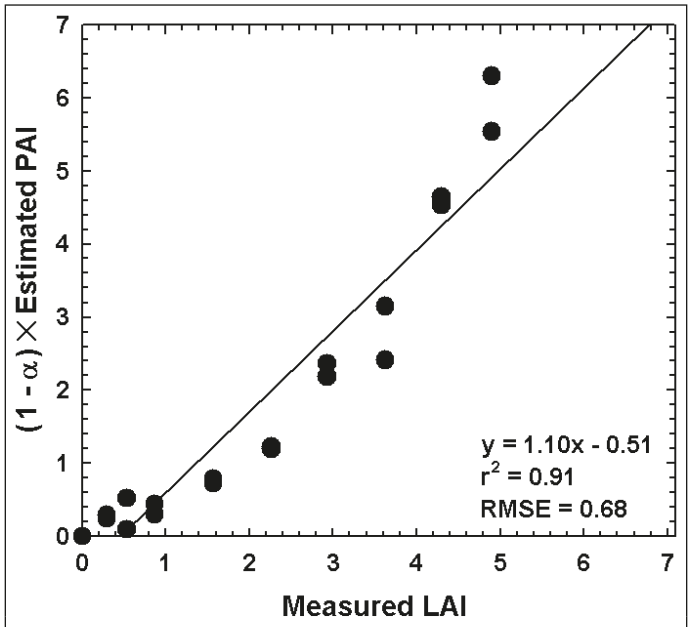

Figure 10. Removal of woody material index, as obtained from leaf-off measurements, using ILRIS-3D improved LAI retrieval accuracies.

characterization of the tree with zero foliage. At a field setting, however, it is impractical to defoliate a tree to determine its woody area index. Nonetheless, it may be feasible to acquire field-level lidar scans of broadleaved crowns at the peak of the growing season (leaf-on) and after senescence (leaf-off). However, accounting for changes in the branching structure – woody material index between field measurements could be a challenging task. Alternative approaches that use lidar intensity measurements to separate green from nongreen components could also be explored. Furthermore, there are several obstacles in using TLS in complex forest ecosystems, like the Boreal forest. For example, forests with tall trees with overlapping crowns hinder the ability to acquire crown-specific TLS data, where individual crowns can be separated. Nonetheless, TLS data, especially from a frame-viewing system like the ILRIS-3D, can be used in environments with plantation-like organization for individual crown characterization. For example, research in olive (*Olea europaea* L.) plantations (Moorthy et al., 2007) is revealing that lidar systems are a more

© 2008 CASI

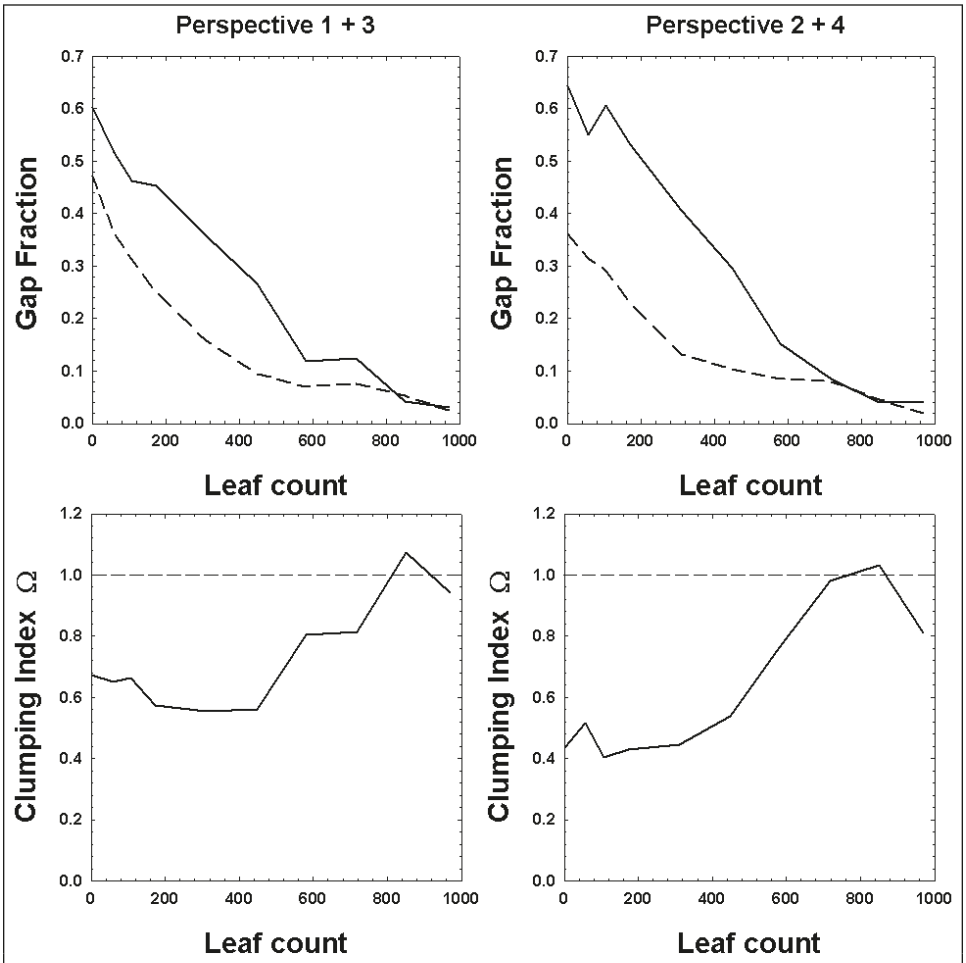

Figure 11. Gap fraction measurements of the artificial tree were compared with gap fraction retrievals from a similar crown with a random distribution of scatterers within the same physical boundary space. Clumping index was determined for the 10 stages of leaf count by examining the relationship between gap fraction of clumped tree (solid line) versus gap fraction of random crown (broken line). Since four perspectives were acquired, the analysis can be repeated for two unique (perspectives 1 + 3 and perspectives 2 + 4), but 3D representations of the tree.

rapid operational approach for acquiring highly detailed crown-specific information as compared to traditional coarse-resolution ground-based survey methods.

Crown-level clumping index

The degree of clumping is a scale-dependent variable. Small-scale clumping depends on the way foliage is located along the stems of an individual plant trunk, whereas large-scale clumping deals with the relative position of plants–trees within a canopy (Weiss et al., 2004). The artificial tree experiment in this investigation provided a unique dataset for directly determining clumping index Ω at the individual plant scale. Since clumping index is evaluated as a deviation from randomness, simulations were conducted to generate randomly distributed elements within the crown. Using the measured return count for the tree from the different perspectives (**Table 4**), random distributions of the equivalent number of returns were produced. The boundary space of the random crown was confined by the limits of the measured values of the *Ficus* crown. The analysis for estimating gap fraction was repeated for the random crowns, and the results were compared with the tree retrievals. It was observed that the gap fraction for the tree (clumped case) was generally greater than the gap fraction for a random crown with the equivalent number of laser pulse returns (**Figure 11**). This finding is in agreement with Chen and Cihlar (1995), who describe that clumped vegetated targets not only have larger gap fractions than random canopies but also exhibit different gap-size distributions. Clumping index profiles as a function of leaf count were calculated using Equation (5) (**Figure 11**). The observed range of clumping index was between 0.43 and 1.07, and the index is near unity at higher leaf counts. Decreasing the number of leaves causes the tree to be more clumped, and subsequently the clumping index deviates from unity. Previously estimated LAI values can now be corrected with the computed clumping indices. The inclusion of the clumping parameter in the LAI estimates further improved LAI retrieval

© 2008 CASI

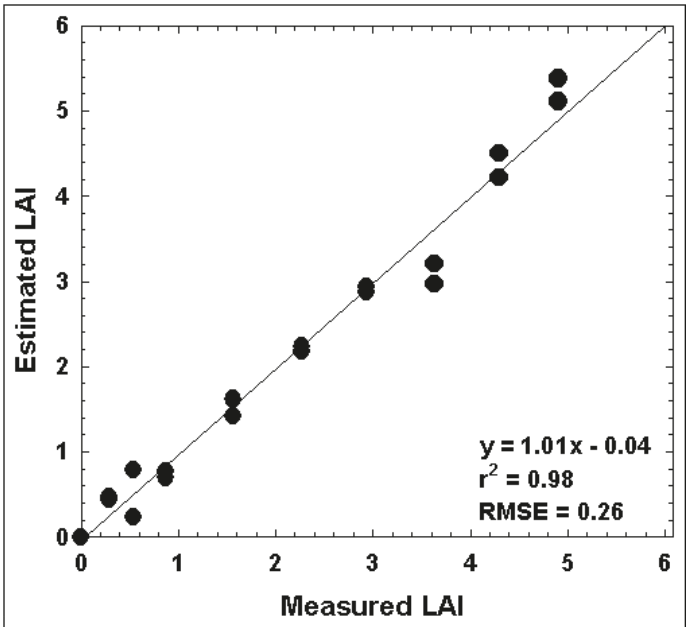

Figure 12. ILRIS-3D-based LAI estimates, now corrected for both woody material and clumping index, are compared with measured LAI from leaf clippings (r^2 = 0.98, RMSE = 0.26).

accuracies (RMSE = 0.26) (**Figure 12**). Furthermore, slope and offset values of 1.01 and –0.04, respectively, indicate the strong linear correlation between lidar-derived LAI estimates and true LAI measurements from destructive sampling.

Conclusion

We have shown that based on laboratory experiments it is feasible to precisely retrieve crown-level structural properties of an individual tree using terrestrial laser scanner (TLS) data. High-resolution laser scans of an artificial tree, with varying degrees of foliage cover, were acquired using the Intelligent Laser Ranging and Imaging System (ILRIS-3D). A slicing-based algorithm was developed to retrieve pertinent information about spatial organization of the measured *XYZ* point cloud datasets. The algorithm was efficient and effective for quantitative analysis and visualization of the laser pulse returns as a function of range distance. Measured laser pulse return densities were compared with theoretical pulse densities (based on sensor intrinsic properties) to compute crown-level gap fraction estimates. Cross-validation of the retrievals revealed strong agreement (r^2 = 0.95), provided that opposing viewpoints of the tree can be merged to overcome the shadowing effect. Subsequent analysis utilized the gap fraction values to determine crown-level leaf area index (LAI). Two major sources of discrepancy in LAI estimation using optically based remote sensing methods are (*i*) the contribution of the woody plant material and (*ii*) the clumping or aggregation of foliage elements. In this investigation both of these discrepancies were quantitatively accounted for through innovative evaluation of the laser point cloud data. The influence of woody plant material was removed using the measured laser pulse return density from the leaf-off state. This correction converts the overestimating plant area index (PAI) values (nongreen + green material) to LAI (only green material). Accounting for the woody material index improved initial PAI estimates with a root mean square error (RMSE) of 1.13 to LAI retrievals with an RMSE of 0.68. The second correction factor or clumping index in this case was determined by comparing the measured spatial distribution of the laser point cloud with a random distribution. Integrating the clumping index factor into the LAI estimates further improved the retrievals (RMSE = 0.26). Based on the results, correcting for the woody material error contribution to LAI estimates was more significant than accounting for the clumping index, for this particular tree. However, determining woody area index in the field setting is not a trivial problem. New methods are being investigated to evaluate if lidar-observed intensity or coupled lidar and multispectral data can offer a potential solution to discern green from nongreen elements within a canopy. Also, to overcome the limitation of using only a single tree in this study, a more extensive benchmark using trees of varying shape and structure will be required to increase confidence in the findings and improve applicability to field-level data. Nonetheless, the experiments described in this study indicate that TLS data are capable of deriving critical crown optical properties (LAI and clumping index) with precision. Such experiments could potentially push the use of TLS data as a viable tool for field-level forest structure characterizations.

Furthermore, current analysis of TLS data includes evaluating the additional benefits of nadir views coupled with traditional tripod-mounted perspectives. ILRIS-3D-derived tree metrics (from multiple perspectives) will be compared with structural retrievals with airborne laser scanners. Also, methodologies are being developed to construct general primitives (i.e., cones, spheres, ellipsoids) from TLS data for use as direct inputs into ray-tracing 3D radiative transfer models. These physically based radiative transfer models have been shown to have particular promise to accurately estimate vegetation canopy biophysical variables in open canopies from remote sensing observations, provided that canopy architecture and scene components are accurately considered. Ongoing research aims to improve the accuracy of 3D radiative transfer models to predict canopy optical characteristics using prior knowledge of the spatial arrangement of vegetated elements at an individual tree scale (i.e., leaves, branches) and at a canopy scale (i.e., plantation, homogeneous, open-clumped) derived from TLS data.

Acknowledgments

This research was made possible by financial support from the Natural Sciences and Engineering Research Council of Canada (NSERC) to J.R. Miller, an NSERC PGS to I. Moorthy, and the availability of the TLS instrumentation funding support to B. Hu by the Canadian Foundation for Innovation (CFI). The authors are most grateful to these funding agencies for their support.

© 2008 CASI

References

Breda, N.J.J. 2003. Ground-based measurements of leaf area index: a review of methods, instruments and current controversies. *Journal of Experimental Botany*, Vol. 54, No. 392, pp. 2403–2417.

Chen, J.M. 1996. Optically-based methods for measuring seasonal variation of leaf area index in boreal conifer stands. *Agricultural and Forest Meteorology*, Vol. 80, pp. 135–163.

Chen, J.M., and Black, T.A. 1992. Defining leaf area index for non-flat leaves. *Plant Cell Environment*, Vol. 15, pp. 421–429.

Chen, J.M., and Cihlar, J. 1995. Plant canopy gap-size analysis theory for improving optical measurements of leaf area index. *Applied Optics*, Vol. 34, No. 27, pp. 6211–6222.

Clawges, R., Vierling, L., Calhoon, M., and Toomey, M. 2007. Use of a ground-based scanning lidar for estimation of biophysical properties of western larch (*Larix occidentalis*). *International Journal of Remote Sensing*, Vol. 28, No. 19, pp. 4331–4344.

Danson, F.M., Hetherington, D., Morsdorf, F., Koetz, B., and Allgower, B. 2007. Forest canopy gap fraction from terrestrial laser scanning. *IEEE Geoscience and Remote Sensing Letters*, Vol. 4, No. 1, pp. 157–160.

Fassnacht, K.S., Gower, S.T., Norman, J.M., and McMurtrie, R.E. 1994. A comparison of optical and direct methods for estimating foliage surface area index in forests. *Agricultural and Forest Meteorology*, Vol. 71, pp. 183–207.

Henning, J.G., and Radtke, P.J. 2006. Detailed stem measurements of standing trees from ground-based scanning lidar. *Forest Science*, Vol. 52, pp. 67–80.

Hopkinson, C., and Chasmer, L.E. 2007. Modelling canopy gap fraction from lidar intensity. In *Proceedings of the ISPRS Workshop on Laser Scanning 2007 and SilviLaser 2007*, 12–14 September 2007, Espoo, Finland. Edited by P. Rönnholm, H. Hyyppä, and J. Hyyppä. pp. 190–195.

Hopkinson, C., Chasmer, L., Young-Pow, C., and Treitz, P. 2004. Assessing forest metrics with a ground-based scanning LiDAR. *Canadian Journal of Forest Research*, Vol. 34, pp. 573–583.

Jonckheere, I., Fleck, S., Nackaerts, K., Muys, B., Coppin, P., Weiss, M., and Baret, F. 2004. Review of methods for in situ leaf area index determination – Part 1: Theories, sensors and hemispherical photography. *Agricultural and Forest Meteorology*, Vol. 121, No. 1, pp. 19–35.

Jonckheere, I., Nackaerts, K., Muys, B., van Aardt, J., and Coppin, P. 2006. A fractal dimension-based modeling approach for studying the effect of leaf distribution on LAI retrieval in forest canopies. *Ecological Modeling*, Vol. 197, No. 1–2, pp. 179–195.

Lang, A.R.G., Yueqin, X., and Norman, J.M. 1985. Crop structure and the penetration of direct sunlight. *Agricultural and Forest Meteorology*, Vol. 35, pp. 83–103.

Lefsky, M.A., Cohen, W.B., Parker, G., and Harding, D. 2002. Lidar remote sensing for ecosystem studies. *Bioscience*, Vol. 52, No. 1, pp. 19–30.

Lichti, D.D., Gordon, S.J., and Stewart, M.P. 2002. Ground-based laser scanners: operation, systems, and applications. *Geomatica*, Vol. 56, pp. 21–33.

Lovell, J.L., Jupp, D.L.B., Culvenor, D.S., and Coops, N.C. 2003. Using airborne and ground-based ranging lidar to measure canopy structure in Australian forests. *Canadian Journal of Remote Sensing*, Vol. 29, No. 5, pp. 607–622.

Moorthy, I., Miller, J.R., Hu, B., Berni, J.A.J., Zarco-Tejada, P., and Li, Q. 2007. Extracting tree crown properties from ground-based scanning laser data. In *IGARSS'07, Proceedings of the International Geoscience and Remote Sensing Symposium*, 23–28 July 2007, Barcelona, Spain. IEEE, Piscataway, N.J. pp. 2830–2832.

Morsdorf, F., Kotz, B., Meier, E., Itten, K.I., and Allgower, B. 2006. Estimation of LAI and fractional cover from small footprint airborne laser scanning data based on gap fraction. *Remote Sensing of Environment*, Vol. 104, pp. 50–61.

Næsset, E. 2002. Predicting forest stand characteristics with airborne scanning laser using a practical two-stage procedure and field data. *Remote Sensing of Environment*, Vol. 80, pp. 88–99.

Neumann, H.H., Hartog, G.D., and Shaw, R.H. 1989. Leaf area measurements based on hemispheric photographs and leaf-litter collection in a deciduous forest during autumn leaf-fall. *Agricultural and Forest Meteorology*, Vol. 45, pp. 325–345.

Parker, G., Lefsky, M., and Harding, D. 2001. Light transmittance in forest canopies determined using airborne laser altimetry and in-canopy quantum measurements. *Remote Sensing of Environment*, Vol. 76, pp. 298–309.

Radtke, P.J., and Bolstad, P.V. 2001. Laser point-quadrat sampling for estimating foliage-height profiles in broad-leaved forests. *Canadian Journal of Forest Research*, Vol. 31, pp. 410–418.

Riano, D., Valladares, F., Condes, S., and Chuvieco, E. 2004. Estimation of leaf area index and covered ground from airborne laser scanner (lidar) in two contrasting forests. *Agricultural and Forest Meteorology*, Vol. 124, No. 2–4, pp. 269–275.

Takeda, T., Oguma, H., Sano, T., Yone, Y., and Fujinuma, Y. 2008. Estimating the plant area density of a Japanese larch (*Larix kaempferi* Sarg.) plantation using a ground-based laser scanner. *Agricultural and Forest Meteorology*, Vol. 148, pp. 428–438.

Thies, M., Pfeifer, N., Winterhalder, D., and Gorte, B.G.H. 2004. Three-dimensional reconstruction of stems for assessment of taper, sweep, and lean based on laser scanning of standing trees. *Scandinavian Journal of Forest Research*, Vol. 19, pp. 571–581.

van der Zande, D., Hoet, W., Jonckheere, I., van Aardt, J., and Coppin, P. 2006. Influence of measurement set-up of ground-based LiDAR for derivation of tree structure. *Agricultural and Forest Meteorology*, Vol. 141, No. 2–4, pp. 147–160.

Watson, D.J. 1947. Comparative physiological studies in growth of field crops. I. Variation in net assimilation rate and leaf area between species and varieties, and within and between years. *Annals of Botany*, Vol. 11, pp. 41–76.

Watt, P., and Donoghue, D. 2005. Measuring forest structure with terrestrial laser scanning. *International Journal of Remote Sensing*, Vol. 26, No. 7, pp. 1437–1446.

Weiss, M., Baret, F., Smith, G.J., Jonckheere, I., and Coppin, P. 2004. Review of methods for in situ leaf are index (LAI) determination — Part 2: Estimation of LAI, errors and sampling. *Agricultural and Forest Meteorology*, Vol. 121, No. 1, pp. 37–53.

Welles, J.M., and Norman, J.M. 1991. Instrument for indirect measurement of canopy architecture. *Agronomy Journal*, Vol. 83, No. 5, pp. 818–825.

© 2008 CASI